Localization Under Random Measurements with Application to Radiation Sources

Nageswara S. V. Rao, Mallikarjun Shankar
Oak Ridge National Laboratory

Jren-Chit Chin, David K. Y. Yau
Purdue University

Yong Yang, Jennifer C. Hou
University of Illinois at Urban-Champaign

Xiaochun Xu, Sartaj Sahni
University of Florida

Abstract—We consider the problem of estimating the location of a target on a plane using random measurements of sensors' distance-differences to the target. The linear algebraic solution to this problem becomes incomplete under random measurement errors, while the geometric method that always returns a solution has been developed only for 3-sensor configurations. We present three methods to extend the geometric method to a larger number of sensors, and compare their performance using simulations. We then consider the case where measurements are not time-synchronized but are independently collected over the same time-window, and present a simulation-based comparison of two localization methods based on mean of estimators and means of measurements, respectively. We describe a method for localizing point radiation sources from intensity measurements which uses the localization as a component. Based on simulation and test-bed results, our estimators' performance improves with the number of sensors, and with mean of estimators method offer a better overall performance.

Index Terms—Distance-difference, point radiation source, detection and localization.

I. INTRODUCTION

Estimation of the location of a target from measurements from distance-differences by a number of sensors is the classical *difference of time-of-arrival* (DTOA) localization problem. This problem has been studied in areas such as tracking in aerospace systems [20], [9], and more recently sensor networks [24], [8] and embedded networked systems [14]. Also, the DTOA localization problem arises as a component of product-form plume identification [15] and low-level radiation detection [16].

The DTOA localization problem has been solved using different approaches. A linear algebraic solution typically involves matrix inversion and solving a quadratic equation [19], [9], while another solution considers the intersection of hyperbolic curves [4]. A recent overview of network-based localization methods may be found in [18], [24], [8], [14]. The geometric DTOA (GDTOA) localization method [17], [23] computes a precision region that contains the target for the special case of three sensors. When more sensors are available, intersections of precision regions of multiple 3-sensor configurations can be used to increase the precision of the location estimation.

Sensor measurements often contain random components due to measurement errors or inherent randomness in the underlying process (such as radiation) or both. Such random components can have drastic effects on DTOA localization methods. It was shown in [17] that under simple random noise conditions, the quadratic equation of [9], [19] may have imaginary roots, which makes the solutions incomplete. While the geometric method is guaranteed to return a solution under random measurements, it is unclear how to handle more than three sensors. Simply computing the intersection of precision regions of 3-sensor configurations may lead to the empty set, thus leading to an incomplete method. On the other hand, the availability of more sensors should in general help the localization, particularly when the measurements contain random components.

In this paper, we present three methods to extend the GDTOA method to allow a larger number of sensors. In each method, we compute multiple estimators using the GDTOA algorithm on a set of 3-sensor configurations, and then compute the final estimator as follows: (a) GDTOA-A computes the mean of the individual estimators, (b) GDTOA-B computes the estimator whose precision region includes the largest number of other estimators, and (c) GDTOA-C selects the estimator whose 3-sensor configuration has the least periphery length. We perform simulations using the uniform random and Poisson distributions, motivated by the nature of radiation sources, and compare the performance of the three methods. While no unilaterally best method is found, GDTOA-A performs well overall. We then consider the case where sensor measurements are not time-synchronized but are independently collected over the same time window. We propose (i) a *mean of estimators* (MoE) method that utilizes GDTOA-A to compute an estimator at each time step, and computes the mean of these estimators, and (ii) a *mean of mea-*

surements (MoM) method that computes the mean of the measurements and invokes GDTOA-A once to obtain the final estimator. Our simulation results show that MOE outperforms MoM in the case of the Poisson distribution, but the performance is mixed in the case of the uniform random distribution.

In the second part of the paper, we address the problem of localizing a point radiation source, which is solved by adapting the DTOA method to $\log$-distance space. The MoE and MoM methods are evaluated using simulations and measurements from a test-bed. These result indicate that performance of these methods improves as more sensors are deployed, and among them MoE offers better overall performance.

The rest of the paper is organized as follows. We solve the DTOA problem and illustrate our solutions using simulation results in Section II. We utilize the developed DTOA solutions to solve the radiation source localization problem in Section III, wherein we present simulation and test-bed results in Sections III-C and III-D, respectively.

II. DTOA WITH RANDOM MEASUREMENTS

Let $S_i = (x_i, y_i)$, $1 \leq i \leq N$, be the locations of N sensors in the Euclidean space R^2. For any point $P = (x, y) \in R^2$, we have the distance $d(P, S_i) = \sqrt{(x - x_i)^2 + (y - y_i)^2}$, for $1 \leq i \leq N$. We define the *distance-difference* δ_{ij} of P from S_i and S_j as

$$\delta_{i,j}(P) = d(P, S_i) - d(P, S_j)$$

for $1 \leq i, j \leq N$. The *DTOA localization* estimates the location of source $S = (x_u, y_u) \in R^2$ from measurements or estimates of $\delta_{i,j}(S)$, $1 \leq i, j \leq k$, which are collected at the same time or within the same time-window. The sensor measurements involve random components such that the estimate $D(S, S_i)$ of $d(S, S_i)$ is a random variable, often of a complex, unknown distribution. The randomness may be due to measurement errors or properties of the underlying process or both. We denote the random distance-difference by

$$\Delta_{i,j}(S) = D(S, S_i) - D(S, S_j).$$

Let $m_{i,1}, m_{i,2}, \ldots, m_{i,T}$ be a sequence of measurements corresponding to $D(S, S_i)$ collected over an observation time window W. We consider two cases: (a) in the *synchronized measurements* case $m_{i,t}$, $1 \leq i \leq N$, are collected at the same time t, and (b) in the *synchronized time-windows* case, the time-windows are synchronized at all sensors, but not necessarily the individual measurements.
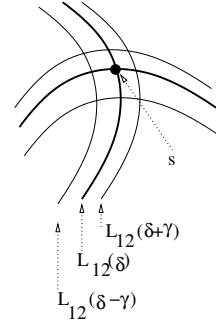

Fig. 1. $R_{S;\gamma}$ is a "distorted" box corresponding to γ-precision region centered at S.

A. Synchronized Measurements

We consider the locus of points defined by

$$L_{i,j}(\delta) = \{P | \delta_{ij}(P) = \delta\}.$$

For the special case of $N = 3$, GDTOA [23], [17] computes the estimate of the target $S = (x_u, y_u)$ by performing a binary search on $L_{1,2}(.)$ to locate $\hat{S} = (\hat{x}_u, \hat{y}_u)$, such that $|\Delta_{1,3}(\hat{S}) - \delta_{13}| \leq \gamma$. The correctness of the binary search is shown by establishing that on $L_{1,2}$ the function $\delta_{1,3}$ varies monotonically so that the binary search can be supported [23].

For any point P on the plane, let $\mathcal{R}_{P,\gamma}$ be the γ-*precision region*, which corresponds to a "distorted box" centered at P, whose sides are formed by displaced hyperbolic curves as shown in Figure II-A. Given synchronized measurements, $m_{i_1,t}, m_{i_2,t}, m_{i_3,t}$, from three sensors, let

$$\hat{S} = (\hat{x}_u, \hat{y}_u) = \mathcal{DTOA}(m_{i_1,t} - m_{i_2,t}, m_{i_1,t} - m_{i_3,t})$$

be the DTOA source location estimate based on measurements from sensors $S_{i_1}, S_{i_2}, S_{i_3}$. When the measurements are exact, i.e. $D(S, S_i) = d(S, S_i)$, for $1 \leq i \leq N$, DTOA ensures that $S \in \mathcal{R}_{\hat{S},\gamma}$. When the measurements are random, one can upper bound the probability that the region $\mathcal{R}_{\hat{S},x}$, for any x, does not contain S, as follows:

$$\begin{aligned}
\mathbf{P}\{S \notin \mathcal{R}_{\hat{S},x}\} &\leq \sum_{j=1}^{3} \mathbf{P}\{D(S, S_{i_j}) > x\} \\
&\leq \frac{1}{x} \sum_{j=1}^{3} E\left[D(S, S_{i_j})\right] \\
&\leq \frac{1}{x} \left(E[D(S_{i_1}, S_{i_2})] + E[D(S_{i_2}, S_{i_3})] \right. \\
&\quad \left. + E[D(S_{i_3}, S_{i_1})]\right).
\end{aligned}$$

The second step of the above derivation uses Chebyshev's Inequality, and the third step uses the triangular inequality of Euclidean distances. For the case of

unbiased measurements, the bound above is given by $\frac{1}{x}\left(d(S_1, S_2) + d(S_2, S_3) + d(S_3, S_1)\right)$, which indicates that tightly packed sensors will give a tighter bound than loosely packed ones.

For $N > 3$, one can invoke GDTOA on 3-combinations of sensors to obtain a number of source estimators $\hat{S}_1, \hat{S}_2, \ldots, \hat{S}_K$, $K \le \binom{N}{3}$. If the measurements are exact, then $\bigcap_{k=1}^{K} \mathcal{R}_{\hat{S}_k, \gamma}$ is guaranteed to contain S, and hence we achieve a good precision. Under random measurements, however, $\bigcap_{k=1}^{K} \mathcal{R}_{\hat{S}_k, \gamma}$ could be the empty set. We propose the following three estimators:

(A) The estimator is given by the mean $\hat{S}_A = \frac{1}{K} \sum_{k=1}^{K} \hat{S}_k$.

(B) The estimator $\hat{S}_B$ maximizes the number of other estimators contained in its precision region such that $\hat{S}_B = \arg\max_{k=1}^{K} \sum_{j=1}^{K} I_{\mathcal{R}_{\hat{S}_k, \gamma}}(\hat{S}_j)$, where $I_A(a)$ is the indicator function that returns 1 if $a \in A$ and 0 otherwise.

(C) The estimator $\hat{S}_C$ is the one with the least circumference for the triangle formed by the three sensors used in computing the estimator.

We simulate a network of sensors in a $[0, 100000] \times [0, 100000]$ grid such that $S_1 = (0, 0)$ and $S_2 = (100000, 0)$. We randomly generate locations of $S_3, \ldots, S_{100}$ on the line segment between $(0, 100000)$ and $(100000, 100000)$. We consider two distributions for measurement errors:

(i) Each sensor measurement corresponds to $(1 + f)r$, where r is the actual distance from the sensor to the source, and f is uniformly randomly generated in the interval $[-F, F]$ for a fixed *multiplicative factor* F. While f values are generated independently, the magnitude of the sensor error is proportional to the distance of sensor from source. By varying F, we can realize different measurement ranges, but the measurements themselves are unbiased since $E[f] = 0$.

(ii) Each sensor measurement is Poisson distributed with the actual distance as the parameter, which gives both the expectation and standard deviation of the distribution. The high variance of the distribution is extensively documented for radiation sources [7], [11], which motivates our study in this paper.

In both cases, the sensor errors are correlated due to the spatial relationships between the sensor locations; a source closer to S_3 generates a smaller error at that sensor and larger errors at S_1 and S_2, which are farther away from the source. Using 100 sensors, the average errors achieved achieved over 1000 measurement sets by the three estimators are plotted in Figure 2 for

	$\hat{S}_A$	$\hat{S}_B$	$\hat{S}_C$
error	22.046383	29.118643	47.937714

TABLE I
AVERAGE ERRORS FOR POISSON MEASUREMENTS.

f	$\hat{S}_A$	$\hat{S}_B$	$\hat{S}_C$
0.1	28.946884	26.524458	31.216803
0.3	74.440262	83.252556	75.771774
0.5	94.567810	104.224464	90.944778
0.7	143.915543	151.576950	147.732925
0.9	192.619690	217.647400	223.640137

TABLE II
AVERAGE ERRORS FOR UNIFORMLY DISTRIBUTED
MEASUREMENTS.

the case of Poisson measurements. In this case, the estimator $\hat{S}_A$ has the best overall performance as shown in Table I. We note, however, that the other estimators perform better in certain specific cases. For the uniform
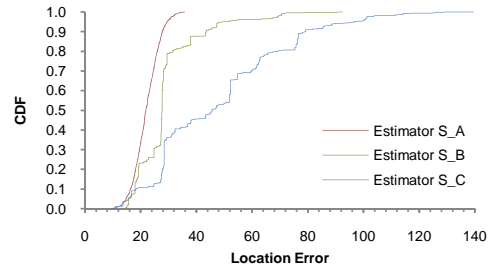

Fig. 2. Errors of the three estimators for Poisson measurements.

distribution model of measurements, the results vary significantly with F. $\hat{S}_A$ has the best overall performance for $F = 0.2, 0.7, 0.9$, while $\hat{S}_B$ and $\hat{S}_C$ perform better for $F = 0.1$ and $F = 0.3$, as shown in Table II. Even in the individual cases, the relative performance of the estimators varies significantly as shown in Figure 3.

B. Synchronized measurement time windows

We now consider two cases in which a sequence of measurements are collected within the same time window at all sensors: (a) the individual sensor measurements are time synchronized, and (b) the individual measurements are not time synchronized. Our objective is to investigate the effects of time synchronization on DTOA, for which we consider the following methods.

(a) *Mean of estimators (MoE):* We are given time synchronized measurements, $m_{1,t}, m_{2,t}, \ldots m_{N,t}$ from sensors $S_1, S_2, \ldots, S_N$, respectively, for $t = 1, 2, \ldots, T$. The MoE method computes the GDTOA-A estimator $\hat{S}_A(t)$ based on $m_{1,t}, m_{2,t}, \ldots m_{N,t}$ at each time step t, and then computes the mean $\hat{S}_{MoE} = \frac{1}{T} \sum_{i=1}^{T} \hat{S}_A(t)$.

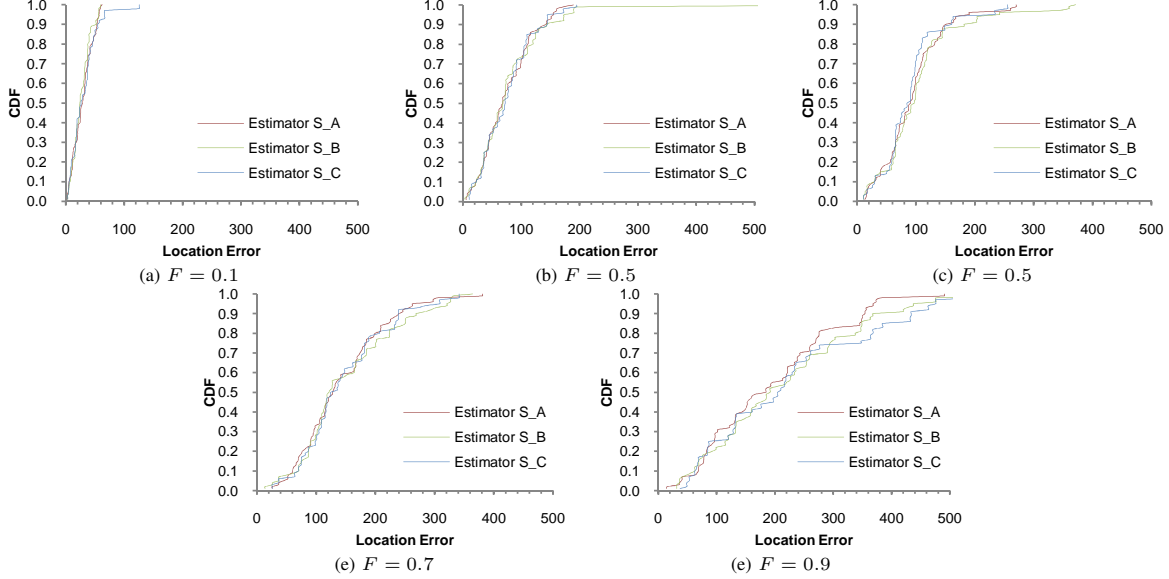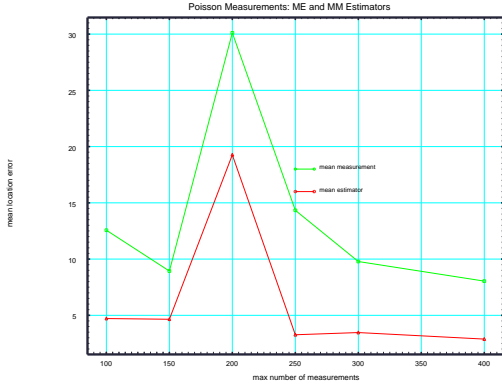Fig. 3. Errors of the three estimators for the uniform distribution of measurements.

Fig. 4. Summary of errors for Poisson measurements.

(b) *Mean of measurements (MoM):* We are given measurements, $m_{1,t_1}, m_{2,t_2}, \ldots m_{N,t_N}$, from sensors $S_1, S_2 \ldots S_N$, respectively, where each t_j takes a value within time-window W. The MoM method utilizes GDTOA-A to compute $\hat{S}_{MoM}$ as the $\hat{S}_A$-estimator using the means of measurements $\bar{m}_1 = \sum_{t_1} m_{1,t_1}$, $\bar{m}_2 = \sum_{t_2} m_{1,t_2}$, $\ldots$, $\bar{m}_N = \sum_{t_N} m_{1,t_N}$.

The overall performance of the MoM and MoE methods is summarized in Figure 4, for the same simulation scenario as in previous section. We generate *error profiles* to quantify the performance of the estimators, wherein we vary the number of sensors N from 5 to 25 in steps

of one and vary the number of measurements T from 10 to 400 in steps of 10. For each value of (N, T), we randomly generate the source, compute $\hat{S}_{MoE}$ and $\hat{S}_{MoM}$, and plot their location errors. MoE performs better in all the cases, since its error surface is below that of $\hat{S}_{MoM}$, as shown in Figure 5 for different values of T. Hence, time synchronization is helpful in the case of Poisson measurements and leads to better localization performance. The error profiles of the MoM and MoE methods for the uniform distribution of measurements are shown in Figure 6 for $T = 400$, where the error magnitude F is varied from 0.1 to 0.9. The performance is mixed in that neither $\hat{S}_{MoE}$ nor $\hat{S}_{MoM}$ is consistently better than the other across the different values of F. In fact, no consistent relative performance is observed even for certain single F values such as $F = 0.5$.

III. LOCALIZATION OF RADIATION SOURCE

We now consider the localization of a point radiation source S of unknown strength A_u expressed in a unit of micro-Curie (μCi) called the *source rate*. The source is located at an unknown location (x_u, y_u). The source gives rise to a radiation intensity of $I(P) = I(x, y) = \frac{A_u E \times 2.22 \times 10^6}{(x_u - x)^2 + (y_u - y)^2}$ (expressed in counts per minute or CPM) when measured by a sensor at point $P = (x, y)$, where E is an efficiency constant unique to the sensor. The radiation count induced by the source and observed at the sensor per unit time is a Poisson random variable with parameter $\lambda = I(x_i, y_i)$, not accounting for the background radiation [7], [11]. Let $B(x, y)$ denote the background radiation strength at (x, y) expressed in CPM, called the *background rate*.
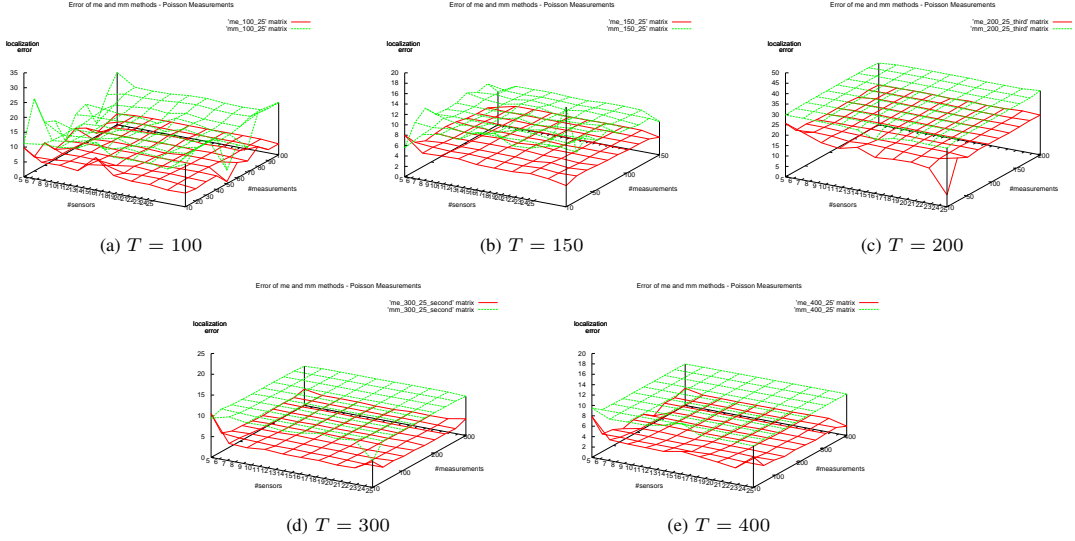
(a) $T = 100$ (b) $T = 150$ (c) $T = 200$

(d) $T = 300$ (e) $T = 400$

Fig. 5. Performance of MoE and MoM methods for Poisson measurements.

(a) $F = 0.1$ (b) $F = 0.4$ (c) $F = 0.5$
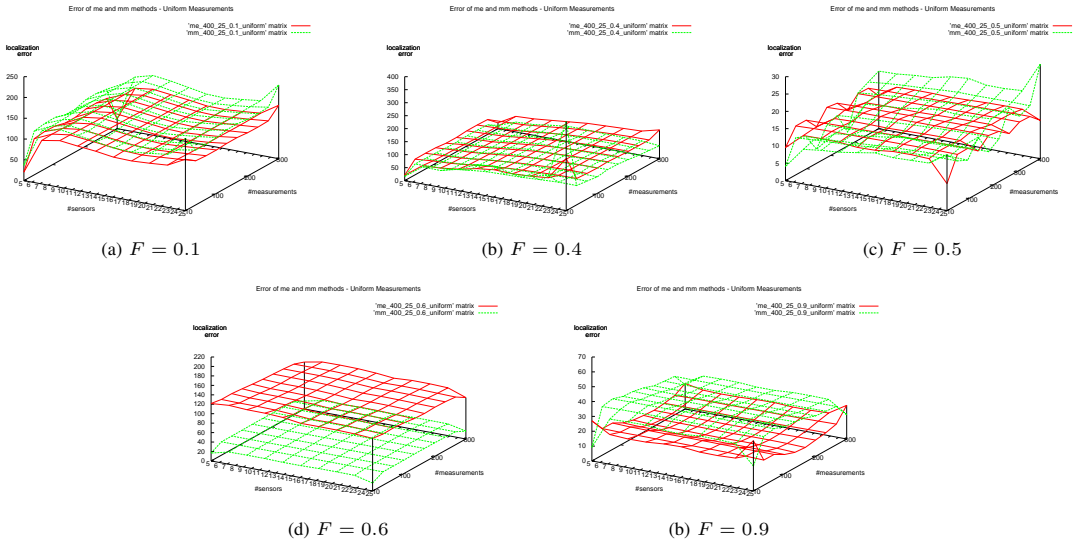
(d) $F = 0.6$ (b) $F = 0.9$

Fig. 6. Performance of MoE and MoM Methods for uniform distribution.

The radiation count measurement (due to the background radiation) at a sensor i located at (x_i, y_i) is given by the Poisson random variable with parameter $B(x_i, y_i)$. The measurements are statistically independent over the temporal dimension, and exhibit significant variations as shown in Figure 7. The use of a network of sensors for detecting and tracking radiation sources has been recently proposed [13], [3], [10], [21], [22], and the problem of localizing a point radiation source has been addressed in [5], [12], [2], [6], [16]. A brief account of these works can be found in [16]. Consider

$$\frac{1}{2} \log \left(\frac{I(S_i)}{I(S_j)} \right) = \log D(S, S_j) - \log D(S, S_i)$$

which is distance-difference in $\log$-space. DTOA has been adapted to $\log$-space to compute $(\hat{x}_u, \hat{y}_u)$ for 3-sensor configurations in [16]. In this section we apply this method to N-sensor configurations along the lines of previous section.

A. Experimental test-bed

We have set up three radiation detection testbeds at (1) the SensorNet Laboratory at Oak Ridge National Laboratory (ORNL), (2) Purdue University, and (3) University of Illinois at Urbana-Champaign. All three testbeds have similar configurations. Figure 8 shows the equipment layout of the test-bed in ORNL. The components of the test-bed include a collection of Rad-CZT radiation
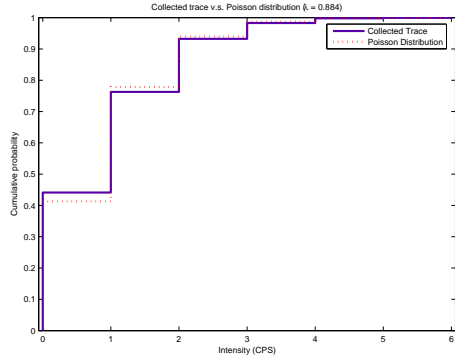
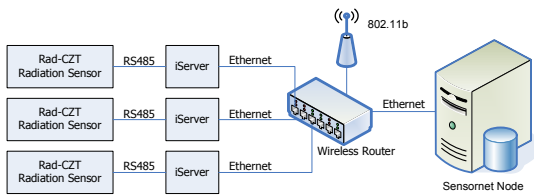Fig. 7.   CDF of measurements from RFTrax radiation sensors.

Fig. 8.   Equipment setup in the radiation test-bed at ORNL.

Sensor	Distance (cm)	Actual (CPM)	Model (CPM)	Estimation Error (CPM)
S_1	13.5	37.0099	48.0821	11.0722
S_1	24.2	21.1236	24.3667	3.2431
S_1	14.0	32.3821	45.6667	13.2846
S_1	23.7	19.9144	24.8235	4.9091
S_1	21.7	22.1469	26.9776	4.8307
S_1	21.5	23.1495	27.2267	4.0772
S_2	22.5	25.3450	28.0667	2.7218
S_2	15.0	38.3307	40.1226	1.7920
S_2	16.3	32.8900	36.7992	3.9093
S_2	14.2	40.3292	42.6366	2.3075
S_2	25.6	24.3019	25.8723	1.5704
S_2	24.1	25.8622	26.8286	0.9665
S_3	20.5	19.7025	20.5222	0.8197
S_3	18.0	21.0433	23.4930	2.4496
S_3	27.0	15.3083	16.2867	0.9784
S_3	19.3	19.5326	21.8044	2.2718
S_3	12.0	35.0893	39.7071	4.6178
S_3	12.3	34.5478	38.3007	3.7529

TABLE IV
ACCURACY OF THE THEORETICAL RADIATION MODEL: ACTUAL
READINGS VERSUS MODEL PREDICTED VALUES.

sensors from RFTrax Inc. [1], a SensorNet node, and a wireless router. Before the experiments, the sensors were calibrated and the efficiency constant E of each sensor was determined. This was done by first collecting a trace of the background radiation, and then another trace with a 0.911 μCi radiation source placed on top of the sensor. E is calculated by

$$E = \frac{(\bar{A} - \bar{B})}{(0.911 \times 2.22 \times 10^6)}$$

where $\bar{A}$ and $\bar{B}$ denote the average intensity of the radiation source and the background intensity, respectively. The calibration is repeated for all the sensors and Table III shows their efficiency constants.

B. Validating the radiation model

We evaluated the accuracy of the radiation model in Section III by laboratory experiments. A 0.911 μCi radiation source was placed some distance away from the three sensors and the readings were collected. The distance between the radiation source and each sensor

Sensor	A	B	E
S_1	4202.69	10.52	0.2078%
S_2	6274.85	13.65	0.3103%
S_3	4882.63	18.42	0.2414%

TABLE III
CALIBRATED EFFICIENCY CONSTANTS OF THE EXPERIMENTAL
RADIATION SENSORS.

was recorded too. The experiment was repeated six times with the radiation source located at different distances from the sensors. A total of 18 traces were collected. The average CPM readings produced at the sensors were compared against the theoretical model and the results are shown in Table IV. The results show that 89% of the time, the value produced by the model is within 5 CPM of the reading collected by the actual sensor.

C. DTOA on simulated radiation sources

We simulate the above radiation intensity model over $[0, 100000] \times [0, 100000]$ grid with $S = (40000, 40000)$, $S_1 = (0, 0)$, $S_2 (100000, 0)$, and $S_3, \ldots S_{1000}$ uniformly distributed on the line segment between $(0, 100000)$ and $(100000, 100000)$. The measurements at S_i are generated as a Poisson random variable with $\lambda_i = I(S_i)$. The errors achieved by the three estimators are plotted in Figure 9, and the average errors are shown in Figure 10 as a function of number of sensors. As in previous section, $\hat{S}_A$ has overall best performance. The performance of $\hat{S}_B$ depends on the precision region, and is quite similar to that of $\hat{S}_A$. $\hat{S}_C$ has the lowest performance in all the cases.

D. Test-Bed Measurements

We arranged the radiation sensors in the testbed to form a triangle. A radiation source (CS-137) of 0.911 μCi is randomly placed inside the triangle formed. We collected six sets of measurements on the testbed, each set containing three traces, thus a total of $N = 18$ traces were collected. Each of the traces has at least 3738 measurements collected at intervals of four seconds. The readings within one set of measurements are synchronized, but the readings are not synchronized across the different sets, which were taken one after another.
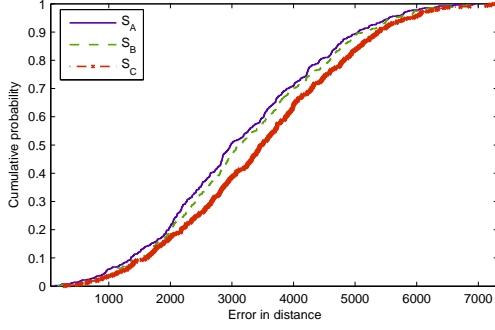
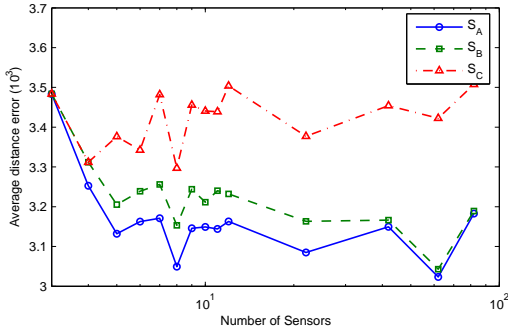Fig. 9. Errors of the three estimators for 500 simulation runs and 10 sensors.

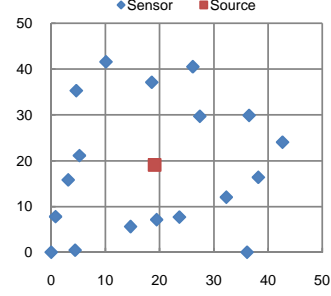Fig. 10. Average error of 500 simulation runs as a function of sensors.

Fig. 11. Sensor and radiation source placements.

(a) MoM

(b) MoE
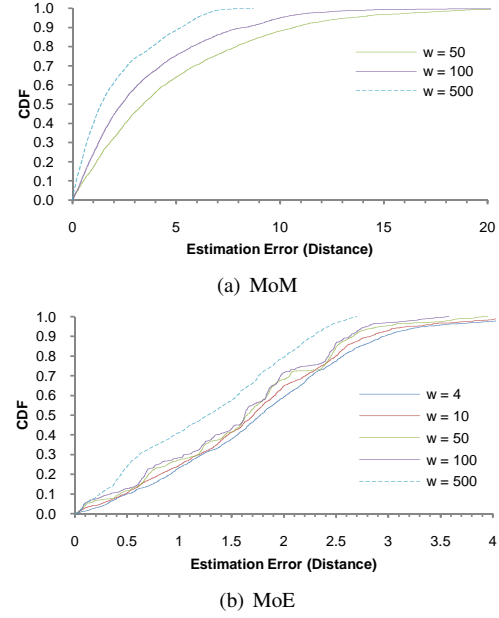
Fig. 12. Performance of DTOA in localizing a radiation point source using 18 sensors.

Using the distances between the radiation source and the sensors, the coordinates of the radiation source and those of the sensors are constructed. We fixed the radiation source at $(19.09, 19.09)$ and placed the sensors accordingly. The locations of the sensors and their distances to the radiation source are summarized in Table V and Figure 11. Using the collected 18 traces of 3738 readings each, we ran the DTOA localization algorithm on each of the $\binom{N}{3}$ combinations of three

Trace ID	1	2	3	4	5	6
Sensor X	36.52	27.45	26.13	18.53	10.11	32.31
Sensor Y	29.89	29.70	40.46	37.08	41.57	12.00
Distance To Source	20.50	13.50	22.50	18.00	24.20	15.00

Trace ID	7	8	9	10	11	12
Sensor X	0.00	5.24	3.13	38.19	4.43	14.65
Sensor Y	0.00	21.09	15.77	16.33	0.47	5.60
Distance To Source	27.00	14.00	16.30	19.30	23.70	14.20

Trace ID	13	14	15	16	17	18
Sensor X	19.46	4.64	36.15	23.65	0.81	42.68
Sensor Y	7.10	35.28	0.00	7.67	7.77	24.01
Distance To Source	12.00	21.70	25.60	12.30	21.50	24.10

TABLE V
SENSOR PLACEMENT.

traces at a time. The position estimates produced by MoM and MoE for each combination are fused by averaging over all the estimates produced. Notice that not all combinations produced an estimate, because the source was too far away from the sensors or it was not contained in the triangle formed by the sensors. The performance statistics of MoM and MoE using 18 sensors are presented in Figure 12. Both MoM and MoE with 18 sensors produce better estimates than with three sensors, and MoE gives better estimates than MoM. For 90% of the time, MoM and MoE produce an estimate that is 10.68 and 2.96 distance units, respectively, away from the actual source position. The results suggest that increasing the number of sensors in the monitoring can reduce the localization error. We systematically quantify the benefits of using more sensors in terms of reduction in the localization error. Using the same 18 traces collected in the previous experiment, we select sets of n traces as input to the DTOA algorithm, where n varies
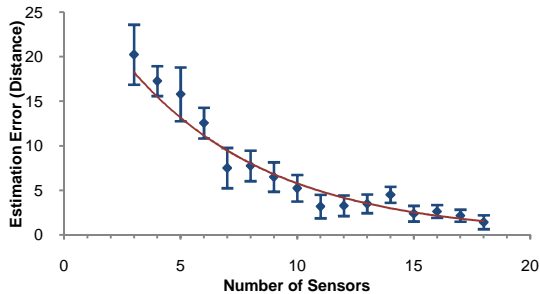
Fig. 13. Estimation error of MoE using different numbers of sensors.

from three to 18 in steps of one. The results are shown in Figure 13, which shows that the performance of MoE improved by utilizing more sensors. In particular, the estimation error is reduced by a factor of 4 by using 10-sensor configuration compared to 3-sensor configuration.

IV. CONCLUSIONS

We considered the problem of estimating the location of a target on a plane using random measurements of distance-differences to it. We compared three methods that extend the geometric method to a larger number of sensors using simulations. We then compared two methods, MoE and MoM, that utilize measurements collected over a time-window. MoE requires time-synchronized measurements but offers a better performance than MoM. We then addressed the problem of localizing a point radiation source by utilizing DTOA method in log-distance space. The MoE and MoM methods are evaluated using simulations and measurements from a test-bed. The results indicate that performance of these methods improves as more sensors are deployed, and MoE offers a overall best performance. In summary, localization problem under random measurements can benefit from having more than 3 sensors, and MoE method offers a good overall solution.

It would be interesting to see if these methods can be analytically compared. Analytical and experimental comparison with other estimators based on linear-algebraic methods would be of interest. More extensive test-bed measurements may be collected to further understand the performance. Further extensions include tracking moving sources and localizing multiple sources.

Acknowledgments

REFERENCES

[1] http://www.rftrax.com/radczt.html.

[2] D. N. Anderson, D. C. Stromswold, S. C. Wunschel, A. J. Peurrung, and R. R. Hansen. Detection and location of Gamma-Ray sources with a modulating coded mask. *Technometrics*, 48(2):252–261, 2006.

[3] S. M. Brennan, A. M. Mielke, and D. C. Torney. Radiation detection with distributed sensor networks. *IEEE Computer*, pages 57–59, August 2004.

[4] B. T. Fang. Simple solutions for hyperbolic and related position fixes. *IEEE Transactions on Systems, Man and Cybernetics-B*, 26(9):748–753, 2005.

[5] A. Gunatilaka, B. Ristic, and R. Gailis. On localisation of a radilogical point source. In *International Conference on Information, Decision and Control*. 2007.

[6] J. W. Howse, L. O. Ticknor, and K. R. Muske. Least squares estimation techniques for position tracking of radioactive sources. *Automatica*, 37:1727–1737, 2001.

[7] G. F. Knoll. *Radiation Detection and Measurement*. John Wiley, 2000.

[8] B. Krishnamachari, editor. *Networking Wireless Sensors*. Cambridge University Press, 2005.

[9] G. Mellen, M. Pachter, and J. Raquet. Closed-form solution for determining emitter location using time difference of arrival measurements. *IEEE Trans. on Aerospace and Electronic Systems*, 39(3):1056–1058, 2003.

[10] A. Mielke, D. Jackson, S. M. Brennan, M. C. Smith, D. C. Torney, A. B. Maccabe, and J.F. Karlin. Radiation detection with distributed sensor networks. In *SPIE Defense and Security Proceedings*, 2005.

[11] D. Mihalas and B. W. Mihalas. *Foundations of Radiation Hydrodynamics*. Courier Dover Publications, 2000.

[12] M. Morelande, B. Ristic, and A. Gunatilaka. Detection and parameter estimation of multiple radioactive sources. In *International Conference on Information Fusion*. 2007.

[13] R. J. Nemzek, J. S. Dreicer, D. C. Torney, and T. T. Warnock. Distributed sensor networks for detection of mobile radioactive sources. *IEEE Transactions on Nuclear Science*, 51(4):1693–1700, 2004.

[14] G. Pottie and W. Kaiser. *Principles of Embedded Networked System Design*. Cambridge University Press, 2005.

[15] N. S. V. Rao. Identification of simple product-form plumes using networks of sensors with rand om errors. In *International Conference on Information Fusion*, 2006.

[16] N. S. V. Rao, M. Shankar, J. C. Chin, D. K. Y. Yau, S. Srivathsan, S. S. Iyengar, Y. Yang, and J. C. Hou. Identification of low-level point radiation sources using a sensor network. In *International Conference on Information Processing in Sensor Networks*, 2008.

[17] N. S. V. Rao, X. Xu, and S. Sahni. A computational geometric method for dtoa triangulation. In *International Conference on Information Fusion*, 2007.

[18] A. H. Sayed, A. Tarighat, and N. Khajehnouri. Network-based wireless location. *IEEE Signal Processing Magazine*, pages 24–40, July 2005.

[19] H. C. Schau and A. Z. Robinson. Passive source localization employing intersecting sperical surfaces from time-of-arrival differences. *IEEE Trans. on Acoustics, Speech, and Signal Processing*, 35(8):1223–1225, 1987.

[20] R. Schmidt. A new approach to geometry of range difference location. *IEEE Trans. on Aerospace and Electronic Systems*, 8(3), 1972.

[21] D. L. Stephens and A. J. Peurrung. Detection of moving radiaactive sources using sensor networks. *IEEE Transactions on Nuclear Science*, 51(5):2273–2278, 2004.

[22] A. Sundaresan, P. K. Varshney, and N. S. V. Rao. Distributed detection of a nuclear radiaoactive source using fusion of correlated decisions. In *International Conf. on Information Fusion*, 2007.

[23] X. Xu, N. S. V. Rao, and S. Sahni. A computational geometry method for localization using difference of distances. *ACM Journal on Sensor Networks*, 2008. to appear.

[24] F. Zhao and L. Guibas. *Wireless Sensor Networks*. Elsevier, 2004.